Available online at www.sciencedirect.com
SCIENCE DIRECT®
ELSEVIER
Nuclear Instruments and Methods in Physics Research A 516 (2004) 586–593
NUCLEAR INSTRUMENTS & METHODS IN PHYSICS RESEARCH Section A
www.elsevier.com/locate/nima

Using the Monte Carlo – Library Least-Squares (MCLLS) approach for the in vivo XRF measurement of lead in bone

Weijun Guo[a], Robin P. Gardner[a,*], Andrew C. Todd[b]

[a] *Center for Engineering Applications of Radioisotopes (CEAR), North Carolina State University, Raleigh, NC 27695 7909, USA*
[b] *Community and Preventive Medicine, Mount Sinai School of Medicine, New York, NY 10029-6574, USA*

Received 13 May 2003; accepted 12 August 2003

Abstract

The Monte Carlo – Library Least-Squares (MCLLS) method has been developed by the Center for Engineering Applications of Radioisotopes for various XRF applications of multi-elemental composition analysis and implemented with the CEARXRF code. In the present work, it is successfully applied to the in vivo XRF measurement of lead in bone and benchmarked by the measurement of a plaster of Paris phantom of known lead concentration. It is implicitly assumed that if the approach works for this sample that closely approximates the real problem of interest, it will also work for the real in vivo case when the proper description of the real case is used. Traditional techniques for XRF analysis are reviewed briefly and the full advantages of the MCLLS method are discussed. Simulation results are presented that are in good agreement with experimental results. The applicability of the MCLLS method to the lead in bone measurement is supported by the good fitting results obtained with simulated Monte Carlo elemental library spectra and close agreement between simulated and experimental spectra from a calcium-rich matrix-based calibration standard in a test geometrical configuration.

PACS: 39.30.+w; 32.30.Rj; 32.80.−t

Keywords: In vivo lead in bone measurement; XRF; Least-squares fitting; MCLLS; CEARXRF

1. Introduction and background

It is well known that lead is a toxic material, which accumulates in human bones after ingestion or inhalation [1–3]. An effective in vivo bone lead measurement system needs to be optimized with respect to both the source-sample-detector hardware arrangement and the inverse quantitative determination method for elemental compositions.

For traditional XRF analysis, two steps are required for quantitative determination [4]. The first consists of finding the intensity or intensity ratios of the full-energy X-ray peaks of the elements of interest in the sample. The second is to relate those peak intensities to the elemental weight fractions utilizing matrix-effect correction methods.

One of four methods (spectrum stripping, peak integration, deconvolution, and least-squares

*Corresponding author. Tel.: +1-919-515-3378; fax: +1-919-515-5115.
E-mail address: gardner@ncsu.edu (R.P. Gardner).

0168-9002/$ - see front matter
doi:10.1016/j.nima.2003.09.030

fitting) is presently used for the accomplishment of the first step. Spectrum stripping is not very accurate and is also difficult to use since error accumulates as stripping proceeds. Peak integration and deconvolution are basically different applications of the same principle since both use a detector response model to mathematically find peak intensity. The accuracy of the two methods depends on the accuracy of the detector response model. Limited by its functionality, overlapping peaks cannot be resolved by these two methods and only part of the spectral information is used. The least-squares fitting method solves this problem but introduces the new difficulty of experimental acquisition of elemental library spectra, which is the key requirement for the traditional least-squares fitting method.

The second step in matrix-effect correction can be handled by one of two methods: the empirical coefficients method or the fundamental parameters method. Detailed reviews of the empirical coefficients method can be found in Refs. [5,6]. The disadvantage of this approach lies in the time-consuming and expensive requirements of preparing calibration curves. Quite often, these empirical coefficients are system-specific (i.e. not transferable to other systems). The fundamental parameters method, proposed by Gillam and Heal [7], attempts to model the sample matrix effects with a complete mathematical analysis. In principle, the fundamental parameters method is an absolute method and does not require measurements of standard samples. However, since the calculations are complex, the practical application of this approach usually makes use of pure elemental standards and the ratios of the X-ray intensities from the unknown sample to those from the pure element standard. This is done in order to cancel some of the approximations that are used and fundamental parameters that are required and thus simplify the calculation, rendering the fundamental parameters method, in a strict sense, not absolute.

For the in vivo measurement of bone lead, Cd-109 is commonly employed as the fluorescing source for the lead K X-rays [8–13]. The Cd-109 based K-shell XRF technique is the one that has been most widely adopted by the research community. This technique utilizes the high-energy part of the XRF pulse-height spectra (i.e. Pb K X-rays and coherently scattered Cd-109 γ-rays) for the lead composition determination [14–17].

Fig. 1 shows a spectrum from a lead-doped calibration standard of calcium sulphate [17]. It is clear that the K_α and K_β lead lines lie above the Compton back-scattered background and that the L lines lie among the escape peaks of the Ag X-rays (which arise from the decay of Cd-109), which makes it almost impossible to obtain the Pb L X-ray area information via traditional methods.

With the heuristic idea that better results will be obtained by the use of all the information that is available, the Monte Carlo – Library Least-Squares (MCLLS) method makes the calculation of lead concentration from both K-series X-rays and L-series X-rays. The MCLLS method has been used in EDXRF and Prompt Gamma-Ray Neutron Activation Analysis (PGNAA) [18–22] and its application to XRF analysis was discussed by He [4]. In this paper, we successfully apply this method to the measurement of a plaster of Paris phantom of known lead concentration in a test geometrical configuration. It is implicitly assumed that if the approach works for this sample, it will also work for the real in vivo case.

For completeness, features of CEARXRF are introduced briefly in the following section, which also serves as an introduction to the photon

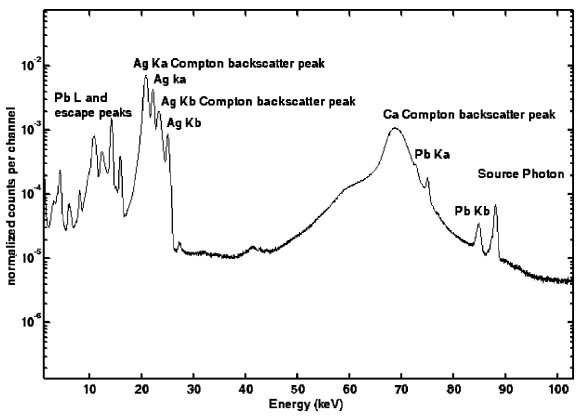

Fig. 1. Low energy Ge detector measurement spectrum with Cd-109 source.

transport modeling for this work. The detailed MCLLS methods for bone lead measurement and results are presented afterwards.

2. The CEARXRF Monte Carlo simulation code

The MCLLS method has been successfully implemented to XRF analysis with the CEARXRF code. This code, an extension of the Monte Carlo code NCSXRF [23] for modeling Energy-Dispersive X-ray Fluorescence (EDXRF) analyzers, has been developed through the implementation of precise low-energy photon transport and XRF physics. One motivation for developing the CEARXRF code was to make it applicable to in vivo XRF system design. For comparison, Table 1 briefly summarizes the features relevant to XRF simulation of the CEARXRF code and widely used general purpose Monte Carlo codes, EGS4 [24], MCNP [25], and ITS [26].

Detailed physics models for photoelectric absorption, incoherent scattering [27] and coherent scattering were coded for both polarized [28–30] and unpolarized photons. The photon cross-sections for all elements ($Z = 1$–94) in the energy range 1–150 keV were taken from the MCNP photon library based on the ENDF/V database [31].

The major component of the background in a bone lead measurement spectrum arises from the Compton scattering of source photons by the sample under measurement. The electron binding effects become apparent in Compton scattering when the photon energy is lower than a few hundred keV. One of the electron binding effects is the Doppler broadening effect in which the Compton-scattered photon energy is broadened by the pre-collision motion of the bound electron [32]. Neglecting this Doppler broadening effect in Compton scattering may result in incorrect Compton scattering profiles in a photon-excited XRF spectrum. A method similar to that in the expanded EGS4 code [29] was adopted to incorporate the Doppler broadening effect into the CEARXRF code. The Hartree-Fock Compton profiles, calculated in the frame of the impulse approximation theory [33], were used to handle the Doppler broadening of Compton-scattered photon energies.

A geometry-modeling package, called HERMETOR [34], was used to characterize the geometry of the EDXRF analyzer for photon tracking. A complex three-dimensional heterogeneous system can be defined by HERMETOR through a simple and verifiable input format. An approach that combined boundary representation and constructive solid geometry techniques [35,36] was employed in this treatment. Information necessary for photon tracking was easily accessible from CEARXRF through calls to subroutines in HERMETOR. The geometry input file can be plotted for any two-dimensional cross-section view (as shown in Fig. 2) with a self-supporting code called HGEMPLOT; a reliable and convenient way to verify the accuracy of the geometry input file.

The CEARXRF code offers several types of source modeling, including excitation sources that

Table 1
Monte Carlo code features for EDXRF simulation

Code	CEARXRF	EGS4	ITS 3.0	MCNP 4C
XRF physics	All K and all L	$K_{\alpha 1}$, $K_{\alpha 2}$, $K_{\beta 1}$, $K_{\beta 2}$ and L	All K and L, average M and N	$K_{\alpha 1}$, $K_{\alpha 2}$, $K_{\beta 1}$, $K_{\beta 2}$ and average L
Photon physics	PE, Incoh, Coh, Doppler polarization	Same with pair	Same without Doppler polarization	Same
Variance reduction	Powerful for XRF	Basically analog	Few and simple	Powerful for transport analog for spectra
Correlated sampling	Yes	No	No	Yes (in 4B)
Library generation	Yes	No	No	No

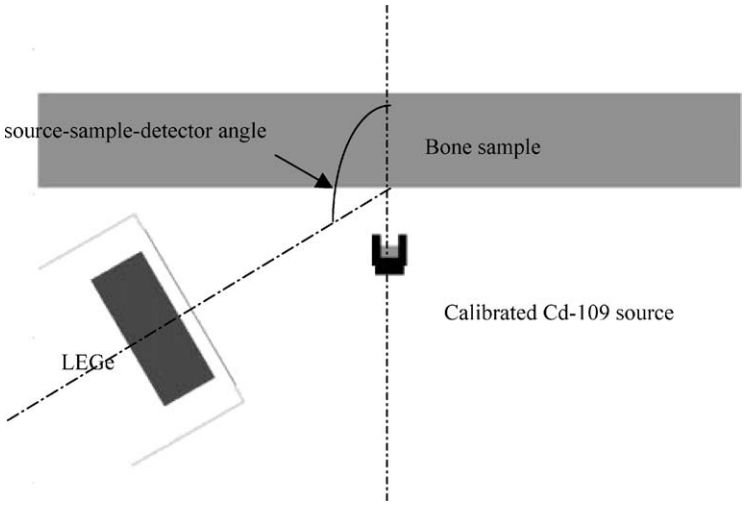

Fig. 2. Geometry for MCLLS simulation.

are commonly used for XRF measurements in practice. This includes radioisotope sources, X-ray tube sources [37], and synchrotron light sources. The excitation can be in either primary or secondary mode. Source photons may be linearly polarized, circularly polarized, or unpolarized. Source photon emission direction can be sampled in a desired direction by a source biasing approach to increase the calculation efficiency for the collimated source-sample geometry.

The XRF pulse-height spectrum was predicted by convolving the detector-incident X-ray spectral flux, simulated by the CEARXRF code, with a detector response function (DRF). A semi-empirical DRF for a Si(Li) detector [38] and a low-energy photon germanium detector [39–41] are presently available with the CEARXRF simulation. These DRF models have the following features: (1) a Gaussian-shaped full-energy peak, (2) a Gaussian-shaped Si or Ge escape peak, (3) a flat continuum from zero to full energy, and (4) an exponential tail located on the low-energy side of the full-energy peak. The values of the model parameters were obtained by nonlinear least-squares fitting of the pulse-height spectra from a number of pure-element samples excited by various radioisotope sources. Simple functional forms of the separable parts of the detected X-ray pulse-height spectrum as functions of incident energy were summed to produce the generalized response function. The detector response function is valid over the range of 5–88 keV for our low-energy photon germanium detector.

The use of variance reduction techniques for Monte Carlo simulation of XRF analyzers needs to take into account the characteristics of analysis as well as the characteristics of photon transport. The major variance reduction techniques in CEARXRF include (1) stratified sampling for sampling all interaction types (photoelectric absorption, incoherent and coherent scatterings) and all characteristic X-rays (K and L) for all elements in the sample if the photon energy is above their absorption edges, (2) statistical estimation of the individual detection probability of a photon directly to the detector at each interaction site, (3) complete composition and density-correlated sampling, and (4) semi-empirical detector response functions.

Complete composition and density-correlated sampling [42,43] is a partially deterministic method which was accomplished by making the normal Monte Carlo calculation on a reference sample and then forcing the same path in a number of comparison samples that contain zones of different composition and density. This was done by making appropriate weight corrections to the comparison samples. These weight corrections

were for distance to collision site and collision element. The additional computation time required to simulate comparison samples is small, typically of the order of 30% for 10 comparison samples containing 15 elements. The correlated sampling feature of CEARXRF is unique and important; it is an excellent way to accurately determine the effect on the XRF measurement of small variations in sample composition and density. Many of the design features of in vivo XRF systems can be investigated by using this technique. More important, this method can be used to obtain calibration curves of XRF systems under a variety of conditions and to study matrix effects in the XRF analysis.

3. The Monte Carlo – library least-squares method

With the MCLLS method, a measured spectrum of an unknown sample is described as a linear combination of library spectra of constituent elements:

$$R_{s,i} = \sum_{j=1}^{n} \alpha_j R_{j,i} + e_i$$

where $R_{j,i}$ is the sample counting rate in the ith channel, α_j is the weight fraction of the jth element in the sample, $R_{j,i}$ is the counting rate in the ith channel contributed by the jth element per unit weight fraction, and e_i is the error term in the ith channel fitting. The weight fractions are obtained by linear least-squares fitting to minimize the reduced χ^2 value with respect to all elements.

$$\chi_v^2 = \frac{1}{v} \sum_{i=n_1}^{n_2} \frac{e_i^2}{\sigma_i^2}$$

where σ_i is the standard deviation of $R_{j,i}$, v is the number of degrees of freedom, and n_1 and n_2 are the limits of the fitting channels. The set of equations for estimation of $\sigma(\alpha_j)$ can be found in the paper by Arinc et al. [44].

As discussed by He [4], the MCLLS method consists of the following steps:

1. By Monte Carlo simulation, the complete pulse-height spectrum is generated for a sample of assumed composition.
2. Within the Monte Carlo computer code, the individual spectral response for each constituent element of the sample is recorded to provide library spectral responses, which is used to generate the library spectra by convolving with detector response function and also Savitsky and Golay polynomial filter to improve the statistics [45].
3. The library least-squares (linear) fitting method is used to obtain the elemental weight fractions in any unknown sample or samples for which the complete spectral response has been measured.
4. If the elemental amounts determined for the unknown sample are not close enough to those assumed for the sample used in the Monte Carlo simulation so that a linear relationship exists, then another Monte Carlo simulation must be performed for an assumed composition closer to the unknown sample or samples. Chi-squared values can be used as an indicator that the correct composition has been found.

The advantages of this method are:

- Elemental library spectra are obtained by Monte Carlo simulation instead of by extensive and time consuming experimental methods.
- Overlapping peaks in the sample spectrum due to X-rays from different elements with close energy values are automatically resolved by this approach.
- The entire spectrum information is utilized.
- The inter-elemental effects are automatically obtained by this approach.
- The measurement uncertainty is directly available from this approach.

To verify the applicability of the MCLLS approach to in vivo bone lead measurement, Monte Carlo simulation was performed (experimental verifications are given in the following experimental results section). The experimental sample was of plaster of Paris, with nominal elemental composition hydrogen (0.6630%), carbon (0.5076%), oxygen (49.9990%), silicon (0.4874%), sulfur (20.8000%), calcium (27.2737%), iron (0.0839%), strontium (0.1691%), and lead (162 μg Pb/g Plaster). The characteristics of the

low energy Germanium detector pertinent to MCLLS are listed in Table 2 [46]. The source-sample-detector angle was $120 \pm 10^{\circ}$, as illustrated in Fig. 2.

The simulated sample spectrum was then fitted with the normalized elemental library spectra to verify that the proper procedure is being used to generate the library spectra, which is a straightforward process as described above.

Table 2
Low energy germanium detector characteristics pertinent to this work

Active crystal area (mm^2)	2000
Active crystal radius (mm)	25.2
Crystal thickness (mm)	15
Window material	Be
Window thickness (mm)	0.5
Window to crystal distance (mm)	5

The simulated sample and library spectra are shown in Fig. 3 and the fitting results are presented in Table 3. With these good fitting results, we are confident that we can apply the library spectra to the fitting of the experimental sample spectrum. This is done in the following section.

4. Experimental results

The experimental spectrum was obtained with the same source-sample-detector arrangement (see Fig. 2) modeled by the simulation. The simulated and experimental spectra are compared in Fig. 4.

Qualitatively, the simulated spectrum shows very good agreement with the experimental spectrum. There are several potential sources of

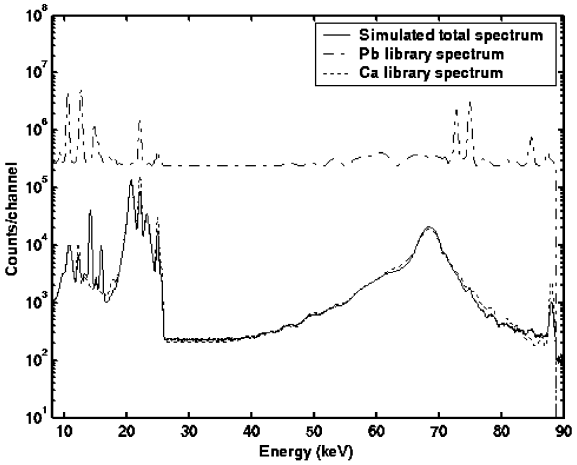

Fig. 3. Simulated total spectrum and library spectra of lead and calcium.

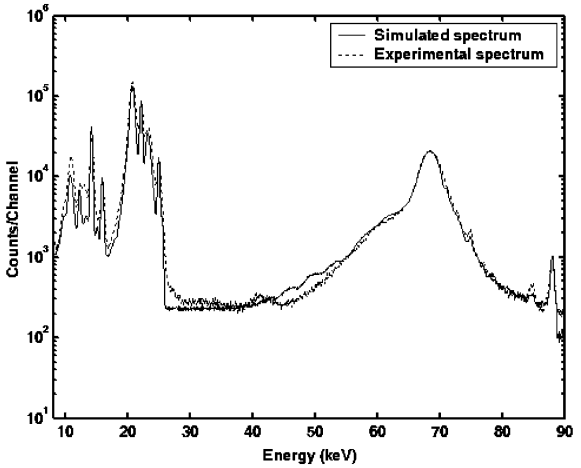

Fig. 4. Simulated sample spectrum compared with the experimental sample spectrum.

Table 3
Library least-squares (LLS) fitting results with simulated sample spectrum

	Calculated weight fraction $\pm$RMS (%)	Nominal weight fraction (%)	Relative error between calculated and nominal values (%)	Correlation coefficient	Reduced χ^2
Ca	27.1073 ± 0.53	27.2737	0.61	0.9660	
Sr	0.1690 ± 0.16	0.1691	0.06	0.2669	1.009
Pb	0.0164 ± 0.94	0.0163	0.61	0.2489	

the discrepancies. These are listed in the order the authors think are most important in the following:

1. Inexact estimation of the background; the background is higher in the high-energy range than it is in the low-energy range.
2. Pulse pile up.
3. Imperfect modeling of the collimator used for the experiment.
4. Error in the semi-empirical model used to estimate the resolution of the detector as a function of energy.
5. Geometry arrangement differences between the experiment and the simulation.

The least-squares fitting was performed by applying simulated elemental library spectra to the experimental spectrum, and the fitting results are presented in Table 4 and Fig. 5. Clearly the fitting results with the simulated sample spectrum are very good and the fitting results with the experimental spectrum show good accuracy also.

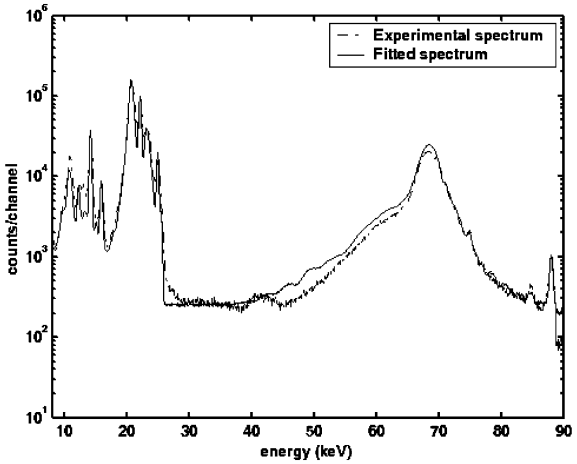

Fig. 5. Least-squares fitted spectrum compared with the experimental sample spectrum.

5. Conclusions, discussion and future work

In this work, the MCLLS technique was applied to the in vivo measurement of lead in bone. The simulated spectrum is in good agreement with the experimental spectrum and the MCLLS-predicted lead concentration of the sample was close to the expected, nominal lead concentration.

To reduce the run time of the simulation code due to inexact 'initial guess' values, we are implementing the differential operator spectrum response to element weight fraction, which will allow adjustment of the simulated spectrum and library spectra by second-order Taylor series expansion. In the de-excitation process of X-ray fluorescence, the lead K-series X-rays and succeeding L-series X-rays are emitted within 10^{-15} s [47]. Based on this fact, coincidence spectroscopy is under investigation to see whether they can be used to improve the bone lead measurement technique.

The authors are developing a software package for the MCLLS application to XRF analysis.

Acknowledgements

The work described was supported by grant number 2R01ES06671 from the National Institute of Environmental Health Sciences, National Institutes of Health, US Public Health Service. Its contents are solely the responsibility of the authors and do not necessarily represent the official views of the NIEHS, NIH.

Table 4
Library least-squares (LLS) fitting results with experimental sample spectrum

	Calculated weight fraction RMS (%)	Nominal weight fraction (%)	Relative error between calculated and nominal values (%)	Correlation coefficient	Reduced χ^2
Ca	24.7316±0.67	27.2737	9.3	0.9068	
Sr	0.1531±0.17	0.1691	9.5	0.2234	303.456
Pb	0.0185±0.96	0.0163	14.2	0.2385	

References

[1] P. Barry, D. Mossman, Br. J. Ind. Med. 27 (1970) 339.
[2] P. Barry, Br. J. Ind. Med. 32 (1975) 119.
[3] P. Barry, Br. J. Ind. Med. 38 (1981) 61.
[4] T. He, Development of the Monte Carlo - library least-squares approach for energy dispersive X-ray fluorescence analysis, Ph.D. Thesis, NCSU, 1992.
[5] R. Jenkins, X-ray Fluorescence Spectrometry, Wiley, New York, 1988.
[6] E.P. Bertin, Principle and Practice of X-ray Spectrometric Analysis, 2nd Edition, Plenum Press, New York, 1975.
[7] E. Gillam, H.T. Heal, Br. J. Appl. Phys. 3 (1952) 358.
[8] D. Chettle, M.C. Scott, K.J. Ellis, W.D. Morgan, In vivo monitoring of trace elements in medicine and research, in: In Vivo Body Composition Studies, IPSM, London, 1987, pp. 300–310.
[9] A. Todd, F. McNeill, J. Palethorpe, D. Peach, D. Chettle, M. Tobin, S. Strosko, J. Rosen, Radiat. Dosim. Stud. Environ. Res. 67 (1992) 117.
[10] S. Green, D. Bradley, J. Palethorpe, D. Mearman, D. Chettle, A. Lewis, P. Mountford, W. Morgan, Phys. Med. Biol. 38 (1993) 389.
[11] A. Aro, A. Todd, C. Amarasiriwardena, H. Hu, Phys. Med. Biol. 39 (12) (1994) 2263.
[12] D. Fleming, D. Chettle, C. Webber, N. Richard, D. Boulay, J.P. Robin, E. O'Flaherty, Br. J. Radiol. 161 (1997) 103.
[13] A.C. Todd, P.J. Parsons, S. Carroll, C. Geraghty, F.A. Khan, S. Tang, E.L. Moshier, Phys. Med. Biol. 47 (2002) 673.
[14] L. Somervaille, D. Chettle, M. Scott, Phys. Med. Biol. 30 (9) (1985) 929.
[15] D. Chettle, M. Scott, L. Somervaille, Environ. Health Perspect. 91 (1991) 49.
[16] C. Gordon, C. Webber, D. Chettle, Environ. Health Perspect. 102 (1994) 690.
[17] A.C. Todd, Phys. Med. Biol. 45 (2000) 1953.
[18] K. Verghese, R.P. Gardner, M. Mickael, C.M. Shyu, T. He, Nucl. Geophys. 2 (1988) 183.
[19] K. Verghese, M. Mickael, T. He, R.P. Gardner, Adv. X-ray Anal. 31 (1989) 461.
[20] T. He, R.P. Gardner, K. Verghese, Appl. Radiat. Isot. 44 (1993) 1381.
[21] C.M. Shyu, R.P. Gardner, K. Verghese, Nucl. Geophys. 7 (1993) 241.
[22] Q. Ao, S.H. Lee, R.P. Gardner, Adv. X-ray Anal. 41 (1999) 922.
[23] T. He, R.P. Gardner, K. Verghese, Adv. X-ray Anal. 35B (1991) 727.
[24] W.R. Nelson, H. Hirayama, D.W.O. Rogers, The EGS4 code system, Stanford linear accelerator center report SLAC-265, 1985.
[25] J.F. Briesmeister (Ed.), MCNP—A general Monte Carlo N-Particle transport code, version 4B, LA-12625-M, LANL, 1997.
[26] J.A. Halbleib, T.A. Mehlhorn, Nucl. Sci. Eng. 92 (1986) 338.
[27] A. Tartari, C. Baraldi, J. Felsteiner, E. Casnati, Phys. Med. Biol. 36 (1991) 567.
[28] Y. Namito, S. Ban, H. Hirayama, Nucl. Instr. and Meth. A 332 (1993) 277.
[29] Y. Namito, S. Ban, H. Hirayama, Nucl. Instr. and Meth. A 349 (1994) 489.
[30] Y. Namito, S. Ban, H. Hirayama, Phys. Rev. A 51 (1995) 3036.
[31] J.S. Hendricks, S.C. Frankle, J.D. Court, ENDF/B-VI Data for MCNP, and errata, Los Alamos National Laboratory report LA-12891, 1994.
[32] B.G. Williams, Compton Scattering, McGraw-Hill, London, 1977.
[33] F. Biggs, L.B. Mendelsohn, J.B. Mann, At. Data Nucl. Data Tables 16 (1975) 201.
[34] T.H. Prettyman, R.P. Gardner, K. Verghese, Nucl. Instr. and Meth. 217 (1990) 465.
[35] J.F. Briesmeister, LANL report LA-7396-M, Rev. 2, 1986
[36] E.A. Straker, W.H. Scott, N.R. Byrn, Defense Nuclear Agency report DNA 2860 T, NTIS, 1972.
[37] P.A. Pella, L. Feng, J.A. Small, X-ray Spectrom. 14 (1985) 125.
[38] T. He, R.P. Gardner, K. Verghese, Nucl. Instr. and Meth. A 299 (1990) 354.
[39] Y. Jin, R.P. Gardner, K. Verghese, Nucl. Instr. and Meth. A 242 (1986) 416.
[40] M.C. Lee, K. Verghese, R.P. Gardner, Nucl. Instr. and Meth. A 262 (1987) 430.
[41] R.P. Gardner, A.M. Yacout, J. Zhang, K. Verghese, Nucl. Instr. and Meth. Phys. Res. A 242 (1986) 399.
[42] R.P. Gardner, M.W. Michael, K. Verghese, Nucl. Geophys. 3 (1989) 157.
[43] R.P. Gardner, M.W. Michael, C.W. Towsley, C.M. Shyu, K. Verghese, IEEE Trans. Nucl. Sci. NS-37 (1990) 1360.
[44] F. Arinc, R.P. Gardner, L. Wielopolski, A.R. Stiles, Adv. X-ray Anal. 19 (1975) 367.
[45] R.v. Grieken, A. Markowicz, Handbook of X-ray Spectrometry, Marcel Dekker, New York, 2002.
[46] Germanium Detectors User's Manual, Canberra Inc., 1998.
[47] J.H. Scofield, At. Data Nucl. Data Tables 14 (1974) 121.